

Results on Diffraction at CDF

Angela Wyatt

On behalf of the CDF Collaboration
 University College London, London WC1E 6BT, UK

Abstract. In run I CDF made an extensive range of measurements studying diffractive processes. In run II these measurements can be extended using improved triggering, new detectors and larger data samples. In these proceedings run II measurements of single diffractive dijet production and double pomeron exchange production of dijets are presented.

1 Introduction

Diffractive events are characterised by a leading (anti-)proton and/or a rapidity gap. These events are associated with the exchange of a strongly interacting colour-singlet object known as the pomeron. Studying diffractive events in the presence of a hard scale, such as that in dijet production, may give an insight into the nature of the exchange.

CDF made an extensive number of diffractive measurements during run I in $p\bar{p}$ collisions ($\sqrt{s} = 1.8$ GeV). In run II ($\sqrt{s} = 1.96$ GeV) these measurements can be extended with larger data-sets, new triggers and improved forward detectors. CDF has built new beam shower counters (BSC) covering $5.5 < |\eta| < 7.5$ and MiniPlug calorimeters covering $3.5 < |\eta| < 5.1$. The roman pots on the out-going anti-proton side are retained from run I.

Figure 1 shows the hit multiplicity in the MiniPlug for diffractive events, selected with the roman pots, and non-diffractive events. There is a good discrimination between the two samples in the zero multiplicity bin where the diffractive signal is concentrated.

In run II CDF have, so far, studied single diffractive dijet production and double pomeron exchange dijet production. Diagrams of these processes are shown in figure 2 and these measurements are now described.

2 Diffractive Dijet Production

Diffractive dijet production, shown in figure 2(a), was measured in run I [1]. The events can be described in terms of a pomeron emitted from the anti-proton, carrying a momentum fraction ξ_p , and a hard scatter between a parton from the pomeron, carrying momentum fraction β , and a parton from the proton. In leading order QCD the ratio of the single diffractive to non-diffractive cross sections is equal to the ratio of the diffractive to anti-proton structure functions.

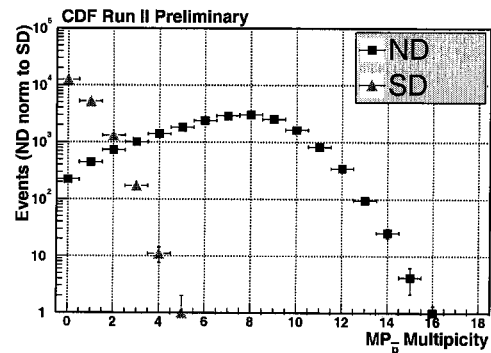


Fig. 1. The MiniPlug hit multiplicity for diffractive events, tagged by the out-going anti-proton in the roman pots, compared to the multiplicity of non-diffractive events.

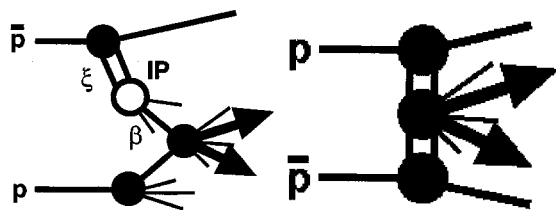


Fig. 2. Diagrams of (a) single diffractive dijet production labeled with the pomeron exchange, IP, and the kinematic variables, and of (b) double pomeron exchange dijet production.

The initial data sample (RP+J5) was collected with a trigger that requires the detection of the leading anti-proton in the roman pots and a calorimeter tower with transverse energy, E_T , of at least 5 GeV. A non-diffractive control sample (J5) requires just the calorimeter tower. Offline, two jets (cone algorithm, $R=0.7$) are required with $E_T^{corr} > 5$ GeV and $|\eta^{jet}| < 2.5$ where the jets are cor-

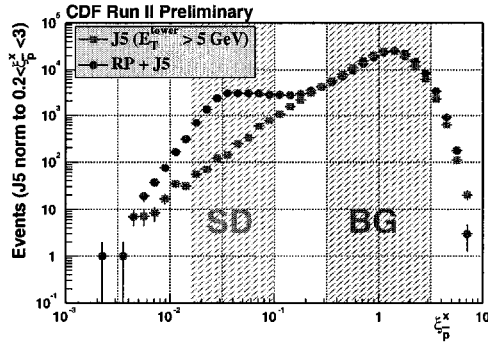


Fig. 3. The $\xi_{\bar{p}}$ distribution of data taken with the RP+J5 trigger compared to data taken with the J5 trigger.

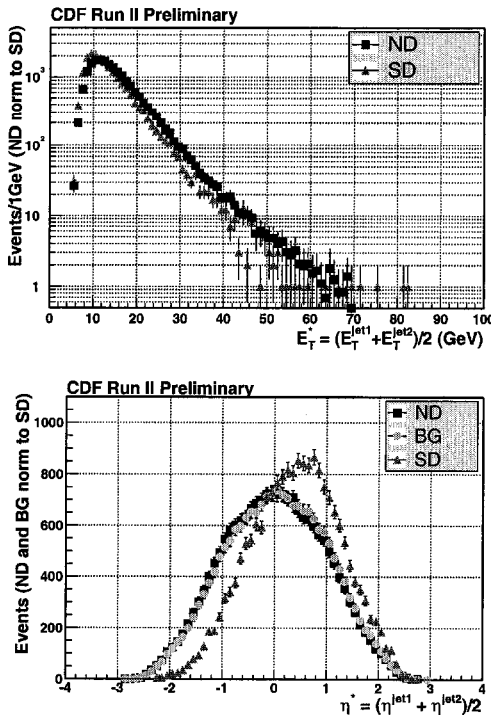


Fig. 4. The average E_T and η of the two highest E_T jets in the SD event sample compared to the ND event sample.

corrected for detector effects and underlying energy. The $\xi_{\bar{p}}$ distributions of the RP+J5 and J5 data samples are compared in figure 3. The two distributions are normalized in the region $0.2 < \xi_{\bar{p}} < 3$, which is away from the diffractive signal with $\xi_{\bar{p}} < 0.1$.

$\xi_{\bar{p}}$ is calculated from summing over all the towers, i , that have $E_T > 100$ MeV and $|\eta| < 5.1$, and $x_{Bj} = \beta\xi$ from summing over the jets, j :

$$\xi_{\bar{p}} = \frac{\sum_i E_T^i e^{-\eta_i}}{\sqrt{s}}, \quad x_{Bj} = \frac{\sum_{jets} E_T^j e^{-\eta_j}}{\sqrt{s}} \quad (1)$$

Roman pot tracking information will also be used to measure $\xi_{\bar{p}}$ in the future. The RP+J5 events are peaked at

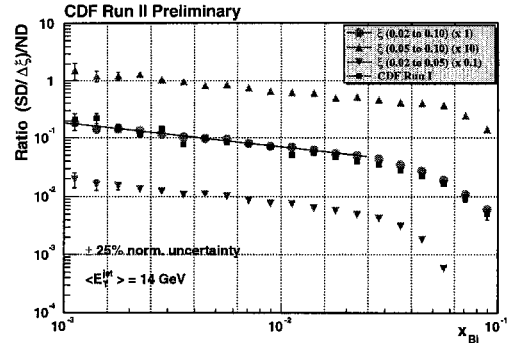


Fig. 5. The ratio of run II SD to ND x_{Bj} distributions compared to run I data; the ratio is also shown for different $\xi_{\bar{p}}$ regions.

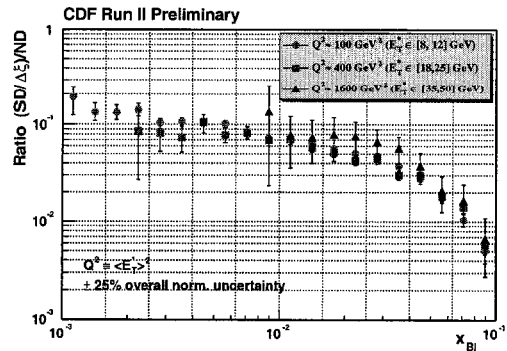


Fig. 6. The ratio of the SD to ND x_{Bj} distributions in different Q^2 regions.

$\xi_{\bar{p}} = 1$; this is due to non-diffractive events overlapping the diffractive events. In the low $\xi_{\bar{p}}$ region ($0.02 < \xi_{\bar{p}} < 0.1$) the distribution is approximately flat as would be expected from diffractive events; the events in this region are selected as the single diffractive (SD) event sample.

The average E_T and η of the jets in the SD sample are compared to those in the non-diffractive (ND) sample in figure 4. The E_T distribution of the SD events is slightly steeper than in the ND event sample, but note that the jets are more forward. The distribution of the average jet rapidity shows that the SD jets are slightly boosted in the direction of the outgoing proton due to the low $\xi_{\bar{p}}$.

The ratio of SD to ND dijets as a function of x_{Bj} is shown in figure 5. The data are in good agreement with run I both in normalisation and shape. The ratio is measured in different $\xi_{\bar{p}}$ ranges and no appreciable $\xi_{\bar{p}}$ dependence is observed. The ratio has also been measured for different $Q^2 = \langle E_T^* \rangle^2$ ranges, figure 6; no significant Q^2 dependence has been observed over the range $100 < Q^2 < 1600$ GeV².

3 Double Pomeron Exchange

The production of dijets by double pomeron exchange was studied in run I [2]. In run II a data-set that is about

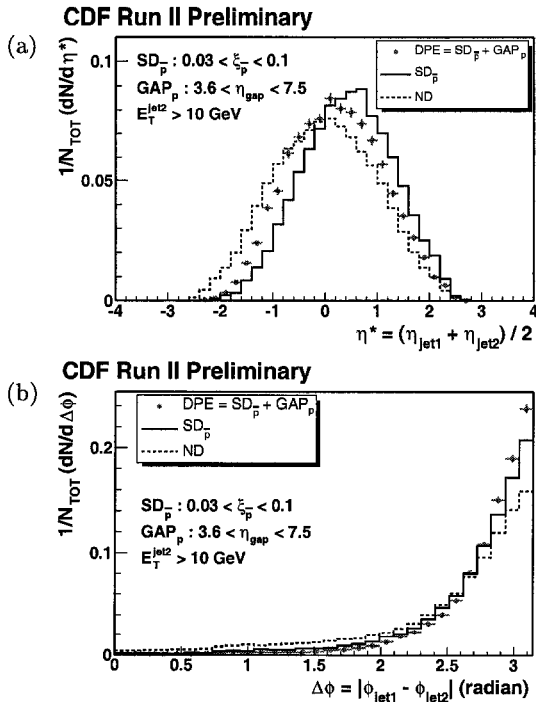


Fig. 7. The average η and the $\Delta\phi$ of the two highest E_T jets in the DPE event sample compared to the SD and ND events.

a factor of 200 larger has already been collected using a dedicated trigger. The trigger requires the detection of the leading anti-proton in the roman pots, a rapidity gap in the BSC on the out-going proton side and a tower of at least 5 GeV in the main calorimeters. Offline, the rapidity gap selection is tightened by requiring a gap in the MiniPlug on the out-going proton side and by selecting $0.03 < \xi_p < 0.1$. Overlapping events are rejected by cutting on the number of vertices, $N_{\text{vertex}} \leq 1$, and cosmics are rejected by demanding there to be no significant missing E_T . At least two jets are required with $E_T^{\text{corr}} > 10 \text{ GeV}$ and $|\eta| < 2.5$. The jets are corrected for detector effects, underlying energy corrections and out-of-cone corrections (from particle-jet to parton energy). The final event sample (the DPE sample) contains around 17,000 events.

The E_T distribution of the jets in the DPE event sample is similar to that in the SD event sample. The average jet η distribution is shown in figure 7(a). The jets are more central than in the SD event sample, now that x_p is more similar to $x_{\bar{p}}$. The dijet $\Delta\phi$ distribution is shown in figure 7(b). The jets are more back-to-back than in the SD event sample in which the jets are more back-to-back than in the ND event sample. This may be due to the suppression of initial state QCD radiation when you replace a coloured parton line with a pomeron.

There has recently been a lot of interest in the possibility that exclusive production may be an interesting search channel for the Higgs boson at the LHC [3]. In exclusive Higgs production no other particles are produced apart from the Higgs and the out-going protons remain intact. Measurements of exclusive dijet production at the Teva-

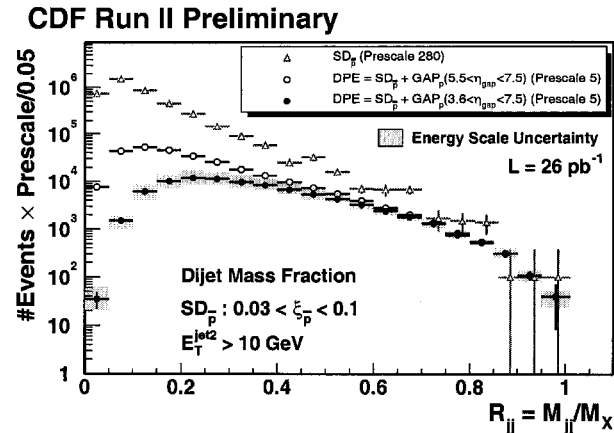


Fig. 8. The dijet mass fraction distribution of the SD event sample and of the DPE event sample, with two different rapidity gap selections.

Table 1. The cross section for $R_{jj} > 0.8$ for a minimum E_T^1 for the DPE sample defined in the text (cone $R=0.7$).

Min E_T^1	Cross Section ($R_{jj} > 0.8$)
10 GeV	970 ± 65 (stat) ± 272 (syst) pb
25 GeV	34 ± 5 (stat) ± 10 (syst) pb

tron can be used to normalise predictions for exclusive Higgs production.

Exclusive dijet events will be characterised by large values of R_{jj} , the ratio of the raw dijet mass measured within the cones $R=0.7$ to the total mass of the central system. Out-of-cone energy causes R_{jj} to be less than one for exclusive events, but still large. The distribution of R_{jj} is shown in figure 8 and is seen to be smoothly falling. The events at large R_{jj} are used to put an upper limit on the cross-section for exclusive dijet production which is given in table 1.

4 Summary

Run II will enable CDF to extend its studies of diffraction. Run II data are in good agreement with run I. The Q^2 dependence of the ratio of the diffractive to non-diffractive structure function has been measured and studies of double pomeron exchange dijet production have been significantly extended. We look forward to a wide range of new and improved measurements from run II.

References

1. T. Affolder *et al.* [CDF Collaboration], Phys. Rev. Lett. **84** (2000) 5043.
2. T. Affolder *et al.* [CDF Collaboration], Phys. Rev. Lett. **85** (2000) 4215.
3. A. De Roeck, V. A. Khoze, A. D. Martin, R. Orava and M. G. Ryskin, Eur. Phys. J. C **25** (2002) 391.